Fundamental Theory of Piezotronics

*Yan Zhang, Ying Liu, and Zhong Lin Wang**

Due to polarization of ions in crystals with noncentral symmetry, such as ZnO, GaN, and InN, a piezoelectric potential (piezopotential) is created in the crystal when stress is applied. Electronics fabricated using the inner-crystal piezopotential as a gate voltage to tune or control the charge transport behavior across a metal/semiconductor interface or a p–n junction are called piezotronics. This is different from the basic design of complimentary metal oxide semiconductor (CMOS) field-effect transistors and has applications in force and pressure triggered or controlled electronic devices, sensors, microelectromechanical systems (MEMS), human-computer interfacing, nanorobotics, and touch-pad technologies. Here, the theory of charge transport in piezotronic devices is investigated. In addition to presenting the formal theoretical frame work, analytical solutions are presented for cases including metal–semiconductor contact and p–n junctions under simplified conditions. Numerical calculations are given for predicting the current–voltage characteristics of a general piezotronic transistor: metal–ZnO nanowire–metal device. This study provides important insight into the working principles and characteristics of piezotronic devices, as well as providing guidance for device design.

1. Introduction

Piezoelectric materials have a wide range of applications in sensors, actuators, and energy harvesting. The most well-known piezoelectric materials are Pb(Zr, Ti)O_3 and quartz. The insulating and non-semiconductive nature of these materials limits their applications in electronic and photonic devices. Recently, much attention has been focused on piezoelectric semiconductor materials in the wurtzite family, including ZnO, GaN, InN, and CdS.[1–7] Due to the coupling of piezoelectric and semiconducting properties, nano- and microwires of piezoelectric semiconductors have been used as basic building blocks for fabricating innovative devices, such as nanogenerators,[8–10] piezoelectric field-effect transistors,[11] piezoelectric diodes,[12] piezoelectric chemical sensors,[13] and piezo-phototronic devices.[14,15] Furthermore, based on the piezoelectric-semiconductor properties, a new field of piezotronics has been created, which uses the effect of the piezoelectric potential created in the crystal for controlling or tuning the charge carrier transport characteristics to fabricate mechanical electronic devices, with potential applications in microelectromechanical systems, nanorobotics, human–computer interfacing, and sensors.[16]

An example is the ZnO nanowire. When a tensile strain is applied along the nanowire that grows in the *c*-axis direction, piezoelectric charges are created at the two ends, forming a piezoelectric potential inside the nanowire. This potential tunes the contact of the nanowire with the electrodes by changing the height of the local Schottky barrier, and, thus, the transport behavior of the charge carriers in the nanowire is controlled and tuned by the externally applied strain. This is the piezotronic effect. The core of piezotronic devices is to utilize the dynamically applied strain to achieve unique mechanical-electronic actions.

Based on the piezoelectric theory and finite element method (FEM), we have previously calculated the piezopotential in a strained ZnO nanowire.[17] Furthermore, considering free carriers in the ZnO crystal, the distribution of piezopotential and carriers have been investigated at thermal equilibrium.[18] These theoretical works have provided a clear description of the distribution of the piezopotential inside a nanowire, but the dynamic transport properties of the carriers in the piezoelectric semiconductor nanowires cannot be described by the static model.

Here, we present a fundamental theoretical framework of piezotronics for understanding and quantitatively calculating the carrier transport behavior in the devices. We first give analytical solutions for ZnO piezoelectric p–n junctions and metal–semiconductor (M–S) contact under simplified conditions, which are useful for understanding the piezotronic behavior in general. Furthermore, using the FEM, the characteristics of a piezotronic transistor ZnO nanowire metal–semiconductor–metal (M–S–M) structure are simulated. The theoretical results establish the basic physics for understanding the observed experimental results from piezotronic devices and guiding future device design.

2. Basic Principle of the Piezotronic Transistor

To illustrate the piezotronic transistor, we begin with a traditional metal oxide semiconductor field-effect transistor (MOS FET). For an n-channel MOS FET (**Figure 1**a), the two n-type doped regions are the drain and source; a thin insulator oxide layer is deposited on the p-type region to serve as the gate

Dr. Y. Zhang, Y. Liu, Prof. Z. L. Wang
School of Material Science and Engineering
Georgia Institute of Technology
Atlanta, Georgia 30332-0245
E-mail: zlwang@gatech.edu

DOI: 10.1002/adma.201100906

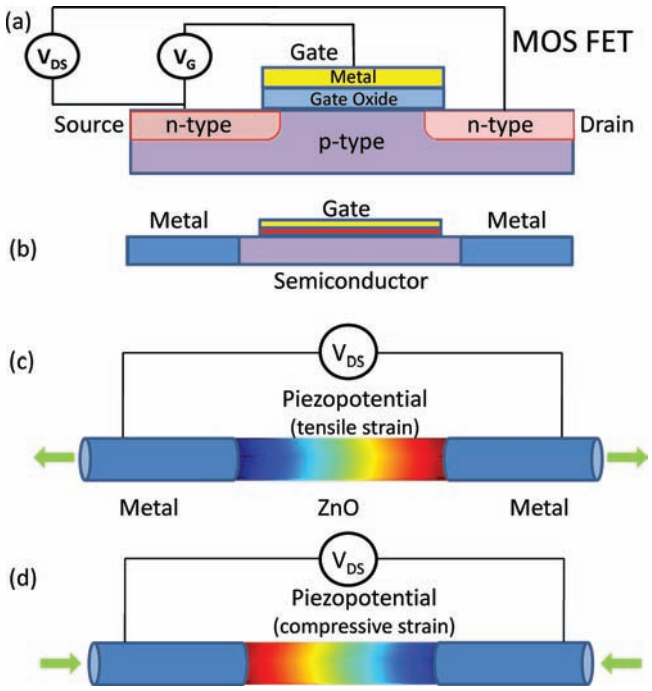

Figure 1. Schematic of a) an n-channel MOS FET and b) a semiconductor nanowire FET. Schematic of a piezotronic transistor with tensile strain (c) and compressive strain (d), where the gate voltage that controls the channel width is replaced by a piezopotential that controls the transport across the M–S interface.

oxide, on which a metal contact is made as the gate. The current flowing from the drain to source under an applied external voltage V_{DS} is controlled by the gate voltage V_G, which controls the channel width for transporting the charge carriers. Analogously, for a single-channel FET fabricated using a semiconductor nanowire (Figure 1b), the drain and source are the two metal electrodes at the two ends, and a gate voltage is applied at the top of the nanowire or through the base substrate. The working principle of the FET is to use an externally applied gate voltage to control the channel width, thus, controlling the charge transport properties.

A piezotronic transistor is a metal–nanowire–metal structure, such as Au–ZnO–Au or Ag–ZnO–Ag, as shown in Figure 1c,d. The fundamental principle of the piezotronic transistor is to control the carrier transport at the M–S interface using a tuning at the local contact by creating a piezopotential at the interface region in the semiconductor by applying a strain. This structure is different from the complimentary metal oxide semiconductor (CMOS) design as described in the following. First, the externally applied gate voltage is replaced by an inner crystal potential generated by the piezoelectric effect, thus eliminating the "gate" electrode. This means that the piezotronic transistor only has two leads: the drain and source. Second, control over channel width is replaced by control at the interface. Since the current transported across a M–S interface is the exponential of the local barrier height in the reversely biased case, the on–off ratio can be rather high due to the non-linear effect. Finally, a voltage-controlled device is replaced by an external strain- or stress-controlled device, which is likely to have complimentary applications to CMOS devices.

Yan Zhang received his B.S. degree (1995) and his Ph.D. in theoretical physics (2004) from Lanzhou University. He worked as a lecturer and associate professor (2007) at the Institute of Theoretical Physics in Lanzhou University. In 2009 he was a research scientist in the group of Professor Zhong Lin Wang at the Georgia Institute of Technology. His main research interests are the dynamics of time-delay systems, complex networks, self-powered nano- and microsystems, and the theoretical calculation of piezotronics.

Ying Liu received her B.S. in physics from the Yuanpei program at Peking University in 2009 and is currently a Ph.D. student with Prof. Z. L. Wang in the Department of Materials Science and Engineering at the Georgia institute of Technology. She is interested in new physics phenomena that are closely related to current energy and electronic applications and is focused on theory and experiments involving the new fields of piezotronics and piezophototronics.

Prof. Zhong Lin (ZL) Wang is the Hightower Chair in Materials Science and Engineering, Regents' Professor, Engineering Distinguished Professor, and Director of the Center for Nanostructure Characterization at the Georgia Institute of Technology. Prof. Wang's research interest include the synthesis, discovery, characterization, and understanding of fundamental physical properties of oxide nanobelts and nanowires, as well as applications of nanowires in energy sciences, electronics, optoelectronics, and biological science. His recent research focuses on the fields of nanogenerators, piezotronics, and piezo-phototronics for fabricating new electronic and optoelectronic devices.

When a ZnO nanowire device is under strain, there are two typical effects that may affect the carrier transport process. One is the piezoresistance effect because of the change in bandgap, charge carrier density, and, possibly, the density of states in the conduction band of the semiconductor crystal under strain.

This effect is a symmetric effect on the two-end contact, has no polarity, and will not produce the function of a transistor. Piezoresistance is a common feature of any semiconductor, such as Si or GaAs, and is not limited to the wurtzite family. The other is the piezoelectric effect because of the polarization of ions in a crystal with noncentral symmetry, which has an asymmetric or non-symmetric effect on the local contacts at the source and drain due to the polarity of the piezopotential. In general, the negative piezopotential side raises the barrier height at the local contact of a metal n-type semiconductor, possibly changing an Ohmic contact to a Schottky contact, a Schottky contact to "insulator" contact. The positive piezopotential side lowers the local barrier height, changing a Schottky contact to an Ohmic contact. The degree of change in the barrier heights depends on the doping type and doping density in the nanowire. The piezoelectric charges are located at the ends of the wire, and thus directly affect the local contacts. The piezotronic effect is likely limited to the wurtzite family, which includes ZnO, GaN, CdS, and InN. It is important to note that the polarity of the piezopotential can be switched by changing tensile strain to compressive strain. Thus, the device can be changed from a control at source to a control at drain simply by reversing the sign of strain applied to the device.[16]

3. Theoretical Framework for the Piezotronic Effect

Since a piezotronic transistor involves a semiconductor that is piezoelectric, the fundamental governing equations for both semiconductor and piezoelectric theories are required. The basic equations for piezotronics are electrostatic equations, current density equations, and continuity equations, which describe the static and dynamic transport behavior of the charge carriers in semiconductors,[19] as well as the piezoelectric equations, which describe the piezoelectric behavior of the material under dynamic strain.[20]

The Poisson equation is the basic equation for describing the electrostatic behavior of charges

$$\nabla^2\psi_i = -\frac{\rho(\vec{r})}{\varepsilon_s} \tag{1}$$

where ψ_i is the electric potential distribution, $\rho(\vec{r})$ is the charge density distribution, and ε_s is the permittivity of the material.

The current-density equations that correlate the local fields, charge densities, and local currents are

$$\begin{cases} \mathbf{J}_n = q\mu_n n\mathbf{E} + qD_n\nabla n \\ \mathbf{J}_p = q\mu_p p\mathbf{E} - qD_p\nabla p \\ \mathbf{J}_{cond} = \mathbf{J}_n + \mathbf{J}_p \end{cases} \tag{2}$$

where $\mathbf{J}_n$ and $\mathbf{J}_p$ are the electron and hole current densities, q is the absolute value of the unit electronic charge, μ_n and μ_p are the electron and hole mobilities, n and p are the concentrations of free electrons and free holes, D_n and D_p are the diffusion coefficients for electrons and holes, $\mathbf{E}$ is the electric field, and J_{cond} is the total current density.

The charge transport driven by a field is described by the continuity equations

$$\begin{cases} \frac{\partial n}{\partial t} = G_n - U_n + \frac{1}{q}\nabla\mathbf{J_n} \\ \frac{\partial p}{\partial t} = G_p - U_p - \frac{1}{q}\nabla\mathbf{J_p} \end{cases} \tag{3}$$

where G_n and G_p are the electron and hole generation rates and U_n and U_p are the recombination rates.

The piezoelectric behavior of the material is described by a polarization vector P. For a small uniform mechanical strain S_{jk},[21] the polarization P vector is given in terms of strain S as

$$(\mathbf{P})_i = (\mathbf{e})_{ijk}(\mathbf{S})_{jk} \tag{4}$$

where the third order tensor $(\mathbf{e})_{ijk}$ is the piezoelectric tensor. According to the conventional theory of piezoelectricity and elasticity,[20,22] the constituter equations can be written as

$$\begin{cases} \sigma = \mathbf{c_E}\mathbf{S} - \mathbf{e}^T\mathbf{E} \\ \mathbf{D} = \mathbf{e}\mathbf{S} + \mathbf{k}\mathbf{E} \end{cases} \tag{5}$$

where σ is the stress tensor, $\mathbf{E}$ is the electric field, $\mathbf{D}$ is the electric displacement, $\mathbf{c_E}$ is the elasticity tensor, and $\mathbf{k}$ is the dielectric tensor.

4. Analytical Solution for 1D Simplified Cases

In practical device modeling, the basic equations presented can be solved under specific boundary conditions. To simply illustrate the basic physics, we consider a 1D piezotronic device with ideal Ohmic contacts at the source and drain. This means that the Dirichlet boundary conditions of the carrier concentration and electrical potential will be applied at the device boundaries.[19] The strain is applied normal to the M–S interface without introducing shear strain.

4.1. Piezoelectric p–n Junctions

The p–n junctions are the most fundamental building blocks in modern electronic devices. The Shockley theory provides a basic theory of the current–voltage (I–V) characteristics of p–n junctions. For a better understanding of a piezoelectric p–n junction, we describe the physics of the semiconductor using the Shockley theory.[19] For simplicity, we assume that the p-type region is non-piezoelectric and n-type region is piezoelectric. Considering that ZnO grows along the direction of c-axis, the positive charges are created at the n-type side of the p–n junction by applying a compressive stress along the c-axis. From convenience piezoelectric theory, the piezoelectric charges are considered as surface charges at the bulk piezoelectric material because the region within which the piezoelectric polarization charges distribute is much smaller than the volume of the bulk crystal, making it reasonable to assume that the piezoelectric charges are distributed at a surface of zero thickness. However, such an assumption is not valid for nanodevices or even microdevices. We assume that the piezoelectric charges distribute at the interface of a p–n junction within a width of W_{piezo} (**Figure 2**a),

We use an abrupt junction model, in which the impurity concentration in a p–n junction changes abruptly from acceptor N_A to donor N_D, as shown in Figure 2a. The electrons and holes in the junction region form a charge depletion zone, which is assumed to have a box profile. We first calculate the

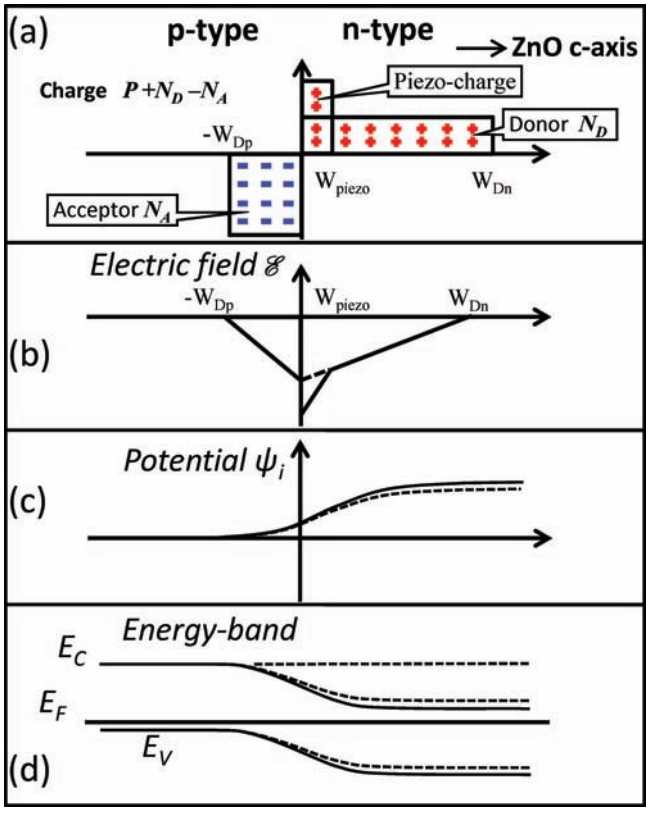

Figure 2. Piezoelectric p–n junction with the presence of piezoelectric charges at applied voltage $V = 0$ (thermal equilibrium). a) Piezoelectric charges and acceptor and donor charge distribution. b) Electric field, c) potential distribution, and d) energy band diagram with the presence of piezoelectric charges. Dashed lines indicate the electric field, potential, and energy band in the absence of piezoelectric charges, and the solid lines indicate the cases when a piezopotential is present at the n-type side.

electric field and potential distribution inside the p–n junction. For a 1D device, the Poisson equation (Equation (1)) may be reduced to

$$-\frac{d^2\psi_i}{dx^2} = \frac{dE}{dx} = \frac{\rho(x)}{\varepsilon_s} = \frac{1}{\varepsilon_s}\left[q N_D(x) - q n(x) - q N_A(x) + q p(x) + q\rho_{piezo}(x)\right] \quad (6)$$

where $N_D(x)$ is the donor concentration, $N_A(x)$ is the acceptor concentration, and $\rho_{piezo}(x)$ is the density of polarization charges (in units of electron charge). W_{Dp} and W_{Dn} are defined as the depletion layer widths in the p-side and the n-side, respectively. The electric field is then obtained by integrating the above equations, as shown in Figure 2b,

$$E(x) = -\frac{q N_A(x + W_{Dp})}{\varepsilon_s}, \text{ for } -W_{Dp} \le x \le 0 \quad (7a)$$

$$E(x) = -\frac{q\left[N_D(W_{Dn} - x) + \rho_{piezo}(W_{piezo} - x)\right]}{\varepsilon_s}, \text{ for } 0 \le x \le W_{piezo} \quad (7b)$$

$$E(x) = -\frac{q N_D}{\varepsilon_s}(W_{Dn} - x), \text{ for } W_{piezo} \le x \le W_{Dn} \quad (7c)$$

The maximum field E_m that exists at $x = 0$ is given by

$$|E_m| = \frac{q(N_D W_{Dn} + \rho_{piezo} W_{piezo})}{\varepsilon_s} \quad (8)$$

The potential distribution $\psi_i(x)$ is, as shown in Figure 2c,

$$\psi_i(x) = \frac{q N_A(x + W_{Dp})^2}{2\varepsilon_s}, \text{ for } -W_{Dp} \le x \le 0 \quad (9a)$$

$$\psi_i(x) = \psi_i(0) + \frac{q}{\varepsilon_s}\left[N_D\left(W_{Dn} - \frac{x}{2}\right)x + \rho_{piezo}\left(W_{piezo} - \frac{x}{2}\right)x\right], \text{ for } 0 \le x \le W_{piezo} \quad (9b)$$

$$\psi_i(x) = \psi_i(W_{piezo}) - \frac{q N_D}{\varepsilon_s}\left(W_{Dn} - \frac{W_{piezo}}{2}\right)W_{piezo} + \frac{q N_D}{\varepsilon_s}\left(W_{Dn} - \frac{x}{2}\right)x, \text{ for } W_{piezo} \le x \le W_{Dn} \quad (9c)$$

Thus, the built-in potential ψ_{bi} is given by

$$\psi_{bi} = \frac{q}{2\varepsilon_s}(N_A W_{Dp}^2 + \rho_{piezo} W_{piezo}^2 + N_D W_{Dn}^2) \quad (10)$$

Equation (10) presents the change in built-in potential as a result of the piezoelectric charges due to tensile or compressive straining, which defines the sign of the local piezoelectric charges. It is apparent that the piezopotential can change the semiconductor energy band relative to Fermi level.

Next, we analyze the current–voltage characteristics of a piezoelectric p–n junction by using the Shockley theory, which models an ideal junction based on four assumptions: 1) a piezoelectric p–n junction has an abrupt depletion layer; 2) piezoelectric semiconductors are nondegenerate so that the Boltzmann approximation applies; 3) the injected minority carrier concentration is smaller than the majority carrier concentration so the low injection assumption is valid; and 4) no generation-recombination current exists inside the depletion layer and the electron and hole currents are constant throughout the p–n junction. If the width of the piezocharges is much less than the width of the depletion zone, e.g., $W_{piezo} << W_{Dn}$, the effect of the piezoelectric charges on the ZnO energy band is considered as a perturbation. The total current density can be obtained by solving Equation (2)[19]

$$J = J_p + J_n = J_0[\exp\left(\frac{qV}{kT}\right) - 1] \quad (11)$$

where the saturation current $J_0 \equiv \frac{q D_p p_{no}}{L_p} + \frac{q D_n n_{po}}{L_n}$, p_{no} is the thermal equilibrium hole concentration in the n-type semiconductor, n_{po} is the thermal equilibrium electron concentration in the p-type semiconductor, and L_p and L_n are diffusion lengths of the electrons and holes, respectively. The intrinsic carrier density n_i is given by

$$n_i = N_C \exp\left(-\frac{E_C - E_i}{kT}\right) \quad (12)$$

where N_C is the effective density of states in the conduction band, E_i is the intrinsic Fermi level, and E_C is the bottom edge of the conduction band.

For a simple case in which the n-type side has an abrupt junction with donor concentration N_D and locally $P_{n0} >> n_{p0}$, then $J_0 \approx \frac{q D_p p_{no}}{L_p}$, and $p_{no} = n_i \exp(\frac{E_i - E_F}{kT})$, so the total current density is given by

$$J = J_0[\exp\left(\frac{qV}{kT}\right) - 1]$$
$$= \frac{q D_p n_i}{L_p} \exp\left(\frac{E_i - E_F}{kT}\right)[\exp\left(\frac{qV}{kT}\right) - 1] \quad (13)$$

If J_{C0} and E_{F0} are defined to be the saturation current density and the Fermi level in the absence of a piezopotential,

$$J_{C0} = \frac{q D_p n_i}{L_p} \exp\left(\frac{E_i - E_{F0}}{kT}\right) \quad (14)$$

According to Equation (9a–c) and Equation (10), the Fermi level E_F in the presence of a piezopotential is given by

$$E_F = E_{F0} - \frac{q^2 \rho_{piezo} W_{piezo}^2}{2\varepsilon_s} \quad (15)$$

Substituting Equation (14) and (15) into Equation (13), we obtain current–voltage characteristics of the piezoelectric p–n junction

$$J = J_{C0} \exp\left(\frac{q^2 \rho_{piezo} W_{piezo}^2}{2\varepsilon_s kT}\right)[\exp\left(\frac{qV}{kT}\right) - 1] \quad (16)$$

This means that the current transported across the p–n junction is an exponential function of the local piezocharges, the sign of which depends on the strain. Therefore, the current to be transported can be effectively tuned or controlled by not only the magnitude of the strain, but also by the sign of the strain (tensile versus compressive). This is the mechanism of the p–n-junction-based piezotronic transistor.

4.2. Metal-Semiconductor Contact

The M–S contact is an important component in electronic devices. Similar to our analysis of the piezoelectric p–n junction, the M–S contact can be simplified in terms of the charge distribution as shown in **Figure 3**a in the presence of a Schottky barrier. The semiconductor side is assumed to be n-type, and the surface states and other anomalies are ignored for simplicity. Under strain, the created piezocharges at the interface not only change the height of the Schottky barrier, but also change its width. Different from the method of changing the Schottky barrier height by introducing dopants at the semiconductor side, the piezopotential can be continuously tuned by strain for a fabricated device.

There are several theories about M–S Schottky contact, including the thermionic-emission theory, diffusion theory, and thermionic-emission-diffusion theory.[19] Although the diffusion model is taken as an example to clearly describe the mechanism of the piezotronic effect in this paper, the presented

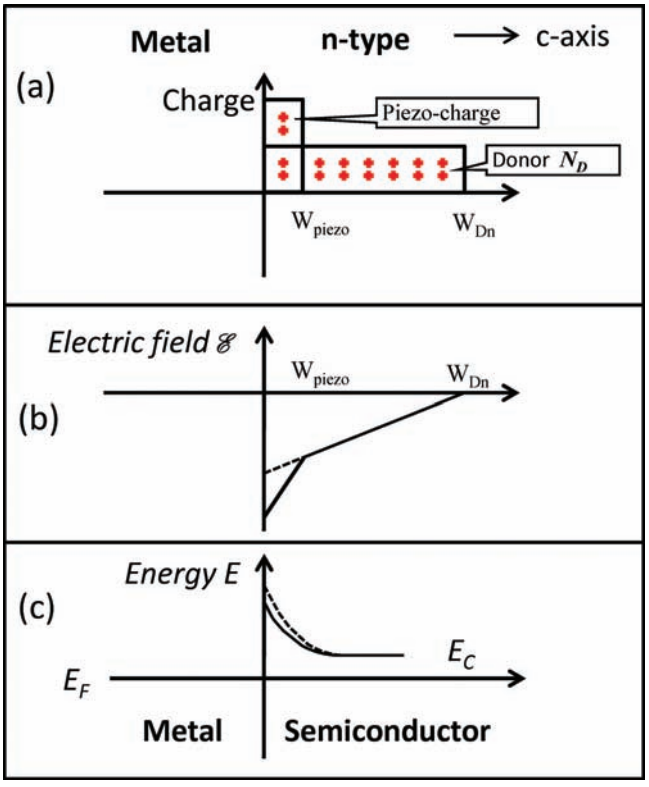

Figure 3. Ideal metal–semiconductor Schottky contacts with the presence of piezoelectric charges at an applied voltage $V = 0$ (thermal equilibrium). a) Space charge distribution. b) Electric field and c) energy band diagram in the presence of piezoelectric charges. Dashed lines indicate the electric field and energy band in the absence of piezoelectric charges and the solid lines indicate the cases when a piezopotential is present in the semiconductor.

methodology also applies to the thermionic-emission and thermionic-emission-diffusion models.

The carriers transport in M–S contact is dominated by the majority carriers. The current density Equation (2) can be rewritten as[19]

$$J = J_n = q\mu_n n E + q D_n \frac{dn}{dx} \quad (17)$$

where $E = \frac{d\psi_i}{dx} = \frac{dE_c}{dx}$.

According to the diffusion theory by Schottky, the solutions under forward bias (a metal is positive bias) can be obtained as[19]

$$J_n \approx J_D \exp\left(-\frac{q\phi_{Bn}}{kT}\right)[\exp\left(\frac{qV}{kT}\right) - 1] \quad (18)$$

where $J_D = \frac{q^2 D_n N_c}{kT}\sqrt{\frac{2q N_D(\psi_{bi} - V)}{\varepsilon_s}} \exp(-\frac{q\phi_{Bn}}{kT})$ is the saturation current density. We define J_{D0} as the saturation current density in the absence of piezoelectric charges

$$J_{D0} = \frac{q^2 D_n N_c}{kT}\sqrt{\frac{2q N_D(\psi_{bi0} - V)}{\varepsilon_s}} \exp\left(-\frac{q\phi_{Bn0}}{kT}\right) \quad (19)$$

where ψ_{bi0} and ϕ_{Bn0} are the built-in potential and Schottky barrier height in the absence of piezoelectric charges. In our

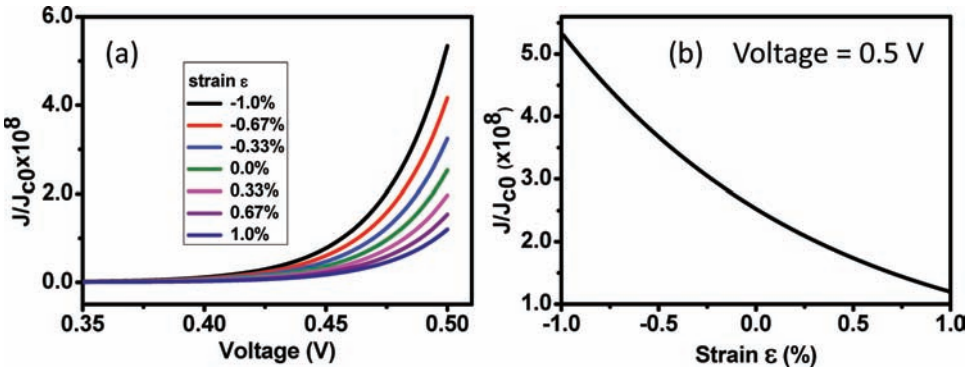

Figure 4. The current–voltage characteristics of an ideal metal–semiconductor Schottky contact in the presence of piezoelectric charges. a) Current–voltage curves at strains ranging from –1% to 1%. b) Relative current density as a function of strain at a fixed forward bias voltage of 0.5 V.

case, the effect of the piezoelectric charge can be considered to be a perturbation to the conduction-band edge E_C. The change in the effective Schottky barrier height induced by piezoelectric charges can be derived from the potential distribution in Equation (9a–c) and Equation (10)

$$\phi_{Bn} = \phi_{Bn0} - \frac{q^2 \rho_{piezo} W_{piezo}^2}{2\varepsilon_s} \tag{20}$$

Thus, the current density can be rewritten as

$$J_n \approx J_{D0} \exp\left(\frac{q^2 \rho_{piezo} W_{piezo}^2}{2\varepsilon_s kT}\right)\left[\exp\left(\frac{qV}{kT}\right) - 1\right] \tag{21}$$

This means that the current transported across the M–S contact is an exponential function of the local piezocharges, the sign of which depends on the strain. Therefore, the current to be transported can be effectively tuned or controlled by not only the magnitude of the strain, but also by the sign of the strain (tensile versus compressive). This is the mechanism of the piezotronic transistor for the M–S case.

4.3. Metal–Wurtzite Semiconductor Contact

We now expand the result presented in Section 4.2 for the special case of a metal–wurtzite semiconductor contact, such as Au–ZnO or Ag–ZnO. For the ZnO nanowire grown along *c*-axis, the piezo-coefficient matrix is written as

$$(e)_{ijk} = \begin{pmatrix} 0 & 0 & 0 & 0 & e_{15} & 0 \\ 0 & 0 & 0 & e_{15} & 0 & 0 \\ e_{31} & e_{31} & e_{33} & 0 & 0 & 0 \end{pmatrix}.$$

If the created strain is strain s_{33} along the *c*-axis, the piezoelectric polarization can be obtained from Equation (4) and (5)

$$P_z = e_{33} s_{33} = q \rho_{piezo} W_{piezo} \tag{22}$$

The current density is

$$J = J_{D0} \exp\left(\frac{q e_{33} s_{33} W_{piezo}}{2\varepsilon_s kT}\right)\left[\exp\left(\frac{qV}{kT}\right) - 1\right] \tag{23}$$

It is clear that the current transported across the M–S interface is directly related to the exponential of the local strain, which means that the current can tuned on or off by controlling the strain.

For numerical calculation, the material constants are the piezoelectric constants $e_{33} = 1.22$ C m^{-2} and the relative dielectric constant is $\varepsilon_S = 8.91$. The width of the piezocharges is $W_{piezo} = 0.25$ nm. The temperature is $T = 300$ K. **Figure 4**a shows the calculated J/J_{D0} as a function of the externally applied voltage V across the M–S interface as a function of the strain, clearly demonstrating its tuning effect on the transported current. When the external voltage is fixed at $V = 0.5$ V at forward bias, J/J_{D0} decreases when the strain changes from –1% to 1% (Figure 4b). The theoretical results agree qualitatively with our previous experiments.[23] For reverse bias case, the dominant voltage dependence is mainly due to the change of the Schottky barrier in our model.

5. Numerical Simulation of Piezotronic Devices

5.1. Piezoelectric p–n Junctions

The analytical solutions for the 1D simplified cases provide qualitative guidance for understanding the mechanism of how the piezopotental tunes and controls the carrier transport behavior. For a general case, the basic equations for the piezotronic device can be solved numerically. For example, with considering the recombination of carriers in the depletion layer, we demonstrate the basic numerical method for simulating the piezoelectric p–n junction.

We first study the DC characteristics of the p–n junction with uniform strain. The piezoelectric charge distribution is received by numerically solving Equation (4) and (5). Then the electrostatic equation, the convection and diffusion equations, and continuity equations are solved using the COMSOL software package. The electrical contacts at the ends of the p–n junction are assumed to be ideal Ohmic contacts and the Dirichlet boundary conditions are adopted for the carrier concentration and electrical potential at the device boundaries.[24] **Figure 5**a shows a sketch of a piezotronic nanowire p–n junction used for the calculation.

In order to have a reasonable comparison to a p–n junction diode, the dopant concentration function N can be approximately described using Gaussian functions

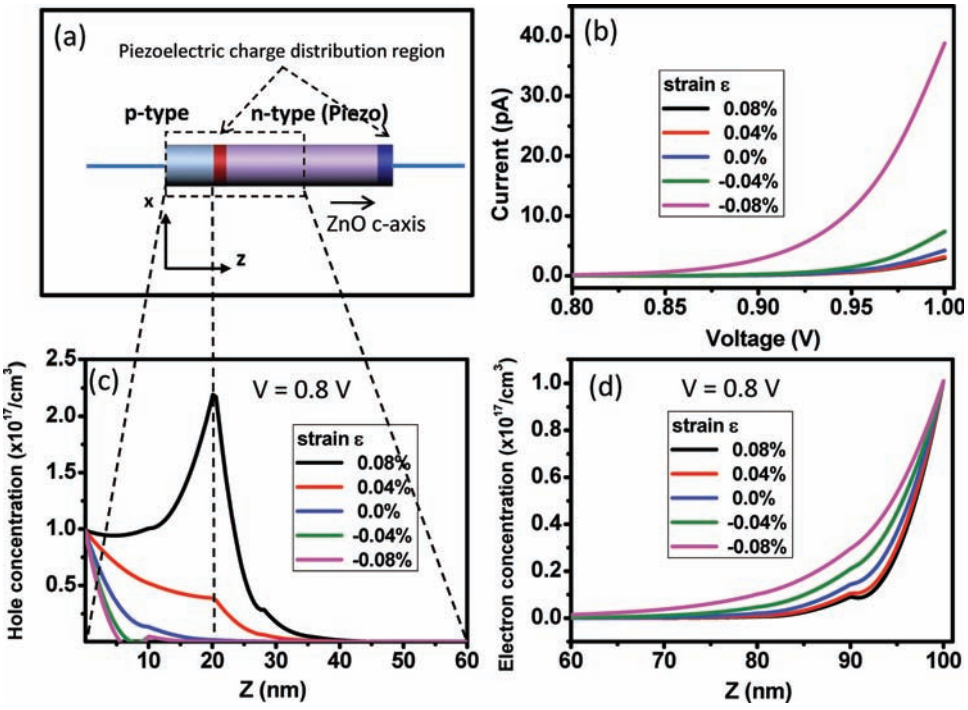

Figure 5. a) Schematic of a piezotronic ZnO nanowire p–n junction. b) Calculated current–voltage curves. c) Distribution of holes and d) distribution of electrons at a fixed forward bias voltage of 0.8 V across the p–n junction under applied strain from –0.09% to 0.09%.

$$N = N_{\mathrm{Dn}} + N_{\mathrm{Dn\ max}} e^{-\left(\frac{z-l}{ch}\right)^2} - N_{\mathrm{Ap\,max}} e^{-\left(\frac{z}{ch}\right)^2} \tag{24}$$

where N_{Dn} is the n-type background doping concentration due to the presence of intrinsic defects, $N_{\mathrm{Dn\ max}}$ is the maximum donor doping concentration, $N_{\mathrm{Ap\ max}}$ is the maximum acceptor doping concentration, l is the length of ZnO nanowire, and ch controls the spreading width of the doping concentration. N is assigned to have a negative value in p-type region and a positive value in n-type region.

There is no external optical excitation in our model, so the electron and hole generation rates $G_{\mathrm{n}} = G_{\mathrm{p}} = 0$. For electron-hole recombination, there are two important recombination mechanisms, including band-to-band recombination and trap-assisted recombination (called Shockley–Read–Hall recombination).[19] Band-to-band recombination describes the energy transition from the conduction band to the valence band by a radiative process (photon emission) or by transfer to another free electron or hole (Auger process). The Shockley–Read–Hall recombination is a general recombination process by traps in the forbidden bandgap of the semiconductor. Taken as an example in our model, the Shockley–Read–Hall recombination is given by

$$U_{\mathrm{p}} = U_{\mathrm{n}} = U_{\mathrm{SRH}} = \frac{np - n_{\mathrm{i}}^2}{\tau_{\mathrm{p}}(n + n_{\mathrm{i}}) + \tau_{\mathrm{n}}(p + n_{\mathrm{i}})} \tag{25}$$

where τ_{p} and τ_{n} are the carrier lifetimes. Thus, the basic semiconductor Equation (1) and (3) are rewritten as

$$\begin{cases} \varepsilon_{\mathrm{s}} \nabla^2 \psi_{\mathrm{i}} = -\ q(p - n + N + \rho_{\mathrm{piezo}}) \\ -\nabla \cdot \vec{J}_{\mathrm{n}} = \quad -\ q\, U_{\mathrm{SRH}} \\ -\nabla \cdot \vec{J}_{\mathrm{p}} = \quad q\, U_{\mathrm{SRH}} \end{cases} \tag{26}$$

For boundaries conditions in contact with a metal electrode, the electrostatic potential is a constant. We assume an infinite recombination velocity and no charge at the contact. Under an applied voltage, the electrostatic potential at the electrode is the potential corresponding to the quasi-Fermi level plus the applied voltage V. The electrostatic potential and carrier concentrator at the electrode are given by[19,25]

$$\psi = V + \frac{q}{kT} \ln\left(\frac{\frac{N}{2} + \sqrt{\left(\frac{N}{2}\right)^2 + n_{\mathrm{i}}^2}}{n_{\mathrm{i}}}\right) \tag{27a}$$

$$n = \frac{N}{2} + \sqrt{\left(\frac{N}{2}\right)^2 + n_{\mathrm{i}}^2} \tag{27b}$$

$$p = -\frac{N}{2} + \sqrt{\left(\frac{N}{2}\right)^2 + n_{\mathrm{i}}^2} \tag{27c}$$

Thus, we can use the above equations to obtain the boundary conditions for the electrostatic potential and carrier concentration at the electrode.

In our simulation, we choose ZnO as the piezoelectric semiconductor material. The length and radius of the nanowire device are 100 nm and 10 nm, respectively. The p-type is assumed to be non-piezoelectric so that it is not restricted to the wurtzite family. For simplicity, we neglect the difference in bandgap between the p-type semiconductor and ZnO. The length of the p-type is 20 nm and the length of n-type ZnO is 80 nm. The relative dielectric constants are $\kappa_{\perp}^{\mathrm{r}} = 7.77$ and $\kappa_{//}^{\mathrm{r}} = 8.91$. The intrinsic carrier density is $n_{\mathrm{i}} = 1.0 \times 10^6\ \mathrm{cm}^{-3}$. The electron and hole mobilities are μ_{n} and $\mu_{\mathrm{p}} = 180\ \mathrm{cm}^2\ \mathrm{V}^{-1}\ \mathrm{s}^{-1}$. The carrier lifetimes are $\tau_{\mathrm{p}} = 0.1\ \mu\mathrm{s}$ and $\tau_{\mathrm{n}} = 0.1\ \mu\mathrm{s}$. The n-type background

doping concentration is $N_{Dn} = 1 \times 10^{15}$ cm^{-3}. The maximum donor doping concentration is $N_{Dn\ max} = 1 \times 10^{17}$ cm^{-3} and the maximum acceptor doping concentration is $N_{Ap\ max} = 1 \times 10^{17}$ cm^{-3}. The control constant $ch = 4.66$ nm. The temperature is $T = 300$ K. The piezoelectric charges are assumed to be distributed uniformly at the two ends of the n-type segment within a region of 0.25 nm, as represented schematically with red and blue colored zones in Figure 5a. For ease of labeling, a z-axis is defined in Figure 5a, with $z = 0$ representing the end of the p-type. The p–n junction is located at $z = 20$ nm along the axis. The n-type ends at $z = 100$ nm.

The current–voltage curves at different strains are shown in Figure 5b. For the negative strain (compressive strain) case in our model, the positive piezoelectric charges are at the p–n interface side and attract the electrons to accumulate near the p–n junction, resulting in a reduction in the built-in potential adjacent to the p–n junction. Thus, the corresponding saturation current density increases at a fixed bias voltage. Alternatively, for the positive strain (tensile strain) case, negative piezoelectric charges are created adjacent to the p–n interface and attract the holes to the local region, resulting in an increase in the built-in potential and a drop in saturation current. Figure 5c shows the distribution of hole concentrations at various strains from –0.08% to 0.08% at an applied voltage of $V = 0.8$ V, displaying the effect of piezoelectric charges on the hole distribution. Under tensile strain, the hole concentration shows a peak directly at the p–n junction interface where the negative piezoelectric charges accumulate. When a compressive strain is applied, the local positive piezoelectric charges push the holes away from the p–n junction, resulting in a disappearance of the peak. Correspondingly, Figure 5d shows the electron distribution in the device at different strains ranging from –0.08% to 0.08% at $V = 0.8$ V, showing a slightly increasing tendency. Since the right-hand electrode is Ohmic contact ($z = 100$ nm), the carriers fully screen the piezoelectric charges at the contact. The electron concentration is rather low adjacent to the p–n junction. The piezoelectric charges at the p–n interface dominate the transport process. Therefore, the piezotronic effect is the result of tuning and controlling the carrier distribution in the device using the generated piezoelectric charges at the two ends.

Using our model, we also studied the DC characteristics and the carrier concentration distribution at various doping concentrations. The strain is fixed at –0.08% and the n-type background doping concentration N_{Dn} is set to 1×10^{15} cm^{-3}. The current–voltage curves that correspond to choosing $N_{Dn\ max} = N_{Ap\ max}$ and increasing $N_{Dn\ max}$ from 1×10^{16} cm^{-3} to 9×10^{16} cm^{-3} are plotted in **Figure 6**a. When the width of the depletion zone is fixed, the built-in potential increases with $N_{D\ max}$. Therefore, the threshold voltage increases, which pushes the "take off" point of the current–voltage curve moves to higher voltage. Then, by assuming $N_{Dn\ max} = N_{Ap\ max} = 1 \times 10^{17}$ cm^{-3} and increasing N_{Dn} from 5×10^{13} cm^{-3} to 1×10^{15} cm^{-3}, the current–voltage curve shows little change, as shown in Figure 6b. The numerical results indicate that the DC characteristics depend on the distributions of the donors and the acceptor doping concentration in the model. Furthermore, the distributions of the holes and electrons at an applied voltage of 0.8 V are shown in Figure 6c,d, respectively.

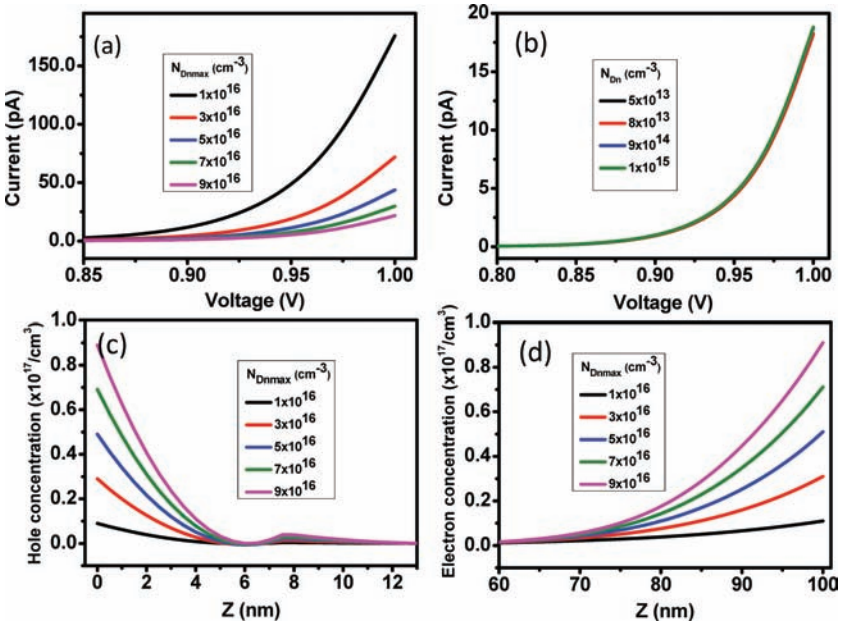

Figure 6. a) Calculated piezoelectric p–n junction current–voltage curves at different maximum donor doping concentrations and maximum donor acceptor doping concentrations. b) Calculated current–voltage curves at various n-type background doping concentration. c,d) Distributions of hole and electron concentrations along the length of the device at an applied forward voltage of 0.8 V at different maximum donor doping concentrations and maximum donor acceptor doping concentrations, respectively.

5.2. Piezoelectric Transistor

The M–S–M ZnO nanowire devices are the typical piezoelectric transistor in our experimental studies. Using the finite element method (FEM), we solved the basic equations of the M–S–M ZnO nanowire device with an applied strain along the nanowire length direction (c-axis). There are many types of M–S–M ZnO nanowire devices, including different types of M–S contacts and doping profiles, etc. The M–S contact can be fabricated as an Ohmic contact or a Schottky contact. The doping profile can be approximated as a box profile, a Gaussian distribution profile, etc. Our calculations are based on a device model that has the following assumptions about the device properties: the surface states in ZnO are ignored; the electrostatic potentials are constant at the end electrodes; the nanowire is n-type without p-type doping; the doping concentration N is approximately described using a Gaussian function; at equilibrium, the electron concentration at the metal contact is unaffected by the transported current; the recombination velocity is infinite; and there is no charge at the contact. Although the M–S–M

ZnO nanowire device model is a simplified model for clearly describing the mechanism of piezopotential tuning the carrier transport process, the basic principle also applies to more complex cases, such as different surface states, arbitrary doping profiles, and different piezoelectric semiconductor materials.

Using the COMSOL software package, the piezoelectric equations (Equation (4)) are solved first. Then, the electrostatic equation and the convection and diffusion equations are solved with the piezoelectric charge distribution provided. The doping concentration function N is approximately descried using a Gaussian function

$$N = N_{\mathrm{Dn}} + N_{\mathrm{Dn\,max}} e^{-\left(\frac{z-l}{ch}\right)^2} \tag{28}$$

The boundary conditions of the electrostatic potential at the electrode can be given by

$$\psi = V - \chi_{\mathrm{ZnO}} - \frac{E_{\mathrm{g}}}{2} + \frac{q}{kT} \ln\left(\frac{\frac{N}{2} + \sqrt{\left(\frac{N}{2}\right)^2 + n_{\mathrm{i}}^2}}{n_{\mathrm{i}}}\right) \tag{29}$$

where the electron affinity χ_{ZnO} of ZnO is 4.5 eV and its bandgap E_{g} is 3.4 eV. By assuming the carrier concentration at the electrode is the same as the value at thermal equilibrium, the boundary conditions of carrier concentration at the electrode can be expressed using Equation (27b).

We calculated the DC transport property of a M–S–M ZnO nanowire device in the presence of piezoelectric charges with applied strain ranging from –0.39% to 0.39%. **Figure 7**a shows a sketch of a piezotronic ZnO nanowire device. We choose l = 50 nm, which is half of the length of the nanowire. The current–voltage curves are shown in Figure 7b. At negative strain (compressive strain), the positive and negative piezoelectric charges are at the left-hand and right-hand M–S contacts, respectively (as shown in Figure 7a), which lower and raise the local Schottky barrier heights at the corresponding contacts. When an external voltage is applied with the left-hand contact at positive bias, the dominant barrier that dictates the current–voltage curve is the reversely biased contact at the right-hand side, at which the local barrier height is raised by piezoelectric charges. Thus, the transported current is lowered in comparison to the case of a strain-free device. Alternatively, in the positive strain (tensile strain) case and under the same bias voltage, the current–voltage curve is largely determined by the M–S contact at the right-hand side, which has a lowered barrier height, resulting in an increase in transported current compared to the strain-free case. The device displays the on state at 0.39% strain, and is off at –0.39% strain. Therefore, the piezopotential acts as a gate voltage to tune and control the current of piezoelectric transistor at the M–S interface and the device can be switched on and off by switching the applied strain, which is the piezotronic FET.

Figure 7c shows the electron concentration along the device at an applied voltage V = 0.8 V. When an external voltage is applied, the piezoelectric charges affect the peak height and position of the electron concentration distribution. With an increase in strain without applying a bias voltage, the magnitude of the peak of the electron concentration increases and the position of the peak shifts from 44.2 nm to 55.8 nm when the strain is varied from –0.39% to 0.39%, as shown in Figure 7d.

Furthermore, we study the DC characteristics and the carrier concentration with different doping concentrations. In order to investigate how variation of the maximum donor doping

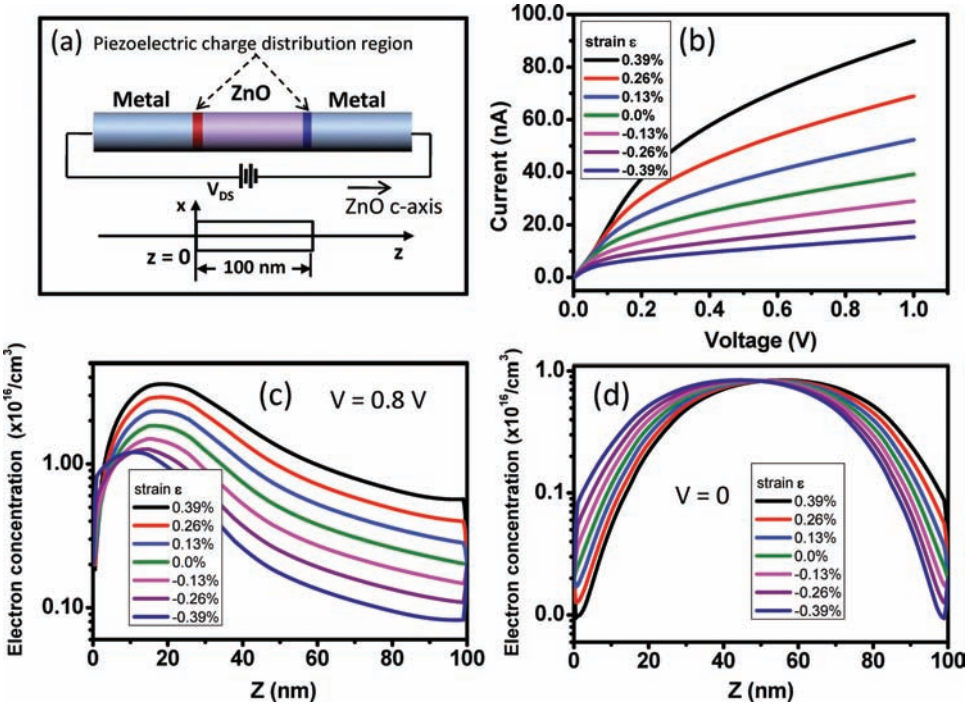

Figure 7. a) Schematic of piezotronic ZnO nanowire transistor. b) Calculated current–voltage curves for the device at different applied strains (–0.39% to 0.39%). The electron distribution in the semiconductor segment c) at a forward voltage V = 0.8 V and d) at V = 0.

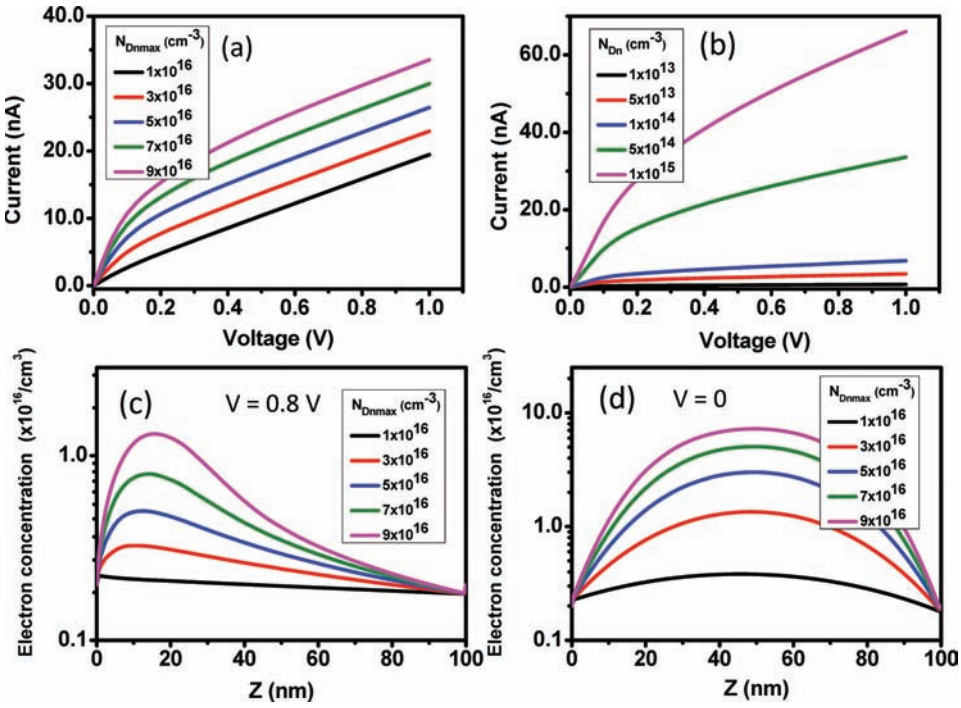

Figure 8. Calculated transport characteristics of a piezotronic ZnO nanowire transistor. a) Piezoelectric M–S–M nanowire transistor current–voltage curves at various maximum donor doping concentrations. b) Current–voltage curves at different n-type background doping concentrations. Calculated electron distribution in the device at differnet maximum donor doping concentrations c) at a forward bias $V = 0.8$ V and d) $V = 0$.

concentration and the maximum donor acceptor doping concentration affects the DC characteristics, we fix the strain at –0.08% and the n-type background doping concentration N_{Dn} of 1×10^{15} cm^{-3}. When $N_{Dn\,max}$ is increased from 1×10^{16} cm^{-3} to 9×10^{16} cm^{-3}, the current increases as well (**Figure 8**a). By fixing $N_{Dn\,max} = N_{Ap\,max} = 1 \times 10^{17}$ cm^{-3}, the current rises with N_{Dn} increasing from 1×10^{13} cm^{-3} to 1×10^{15} cm^{-3} (Figure 8b). The numerical results indicate that the DC characteristics depend on the doping concentration in the piezoelectric transistor. The distribution of electrons at applied voltages of 0.8 V and 0.0 V are shown in Figure 8c,d, respectively.

In summary, we have presented the theoretical frame for piezotronics by studying the charge transport across metal–semiconductor contacts and p–n junctions with the introduction of piezopotential. The analytical solutions derived under simplified conditions are useful for illustrating the major physical characteristics of the piezotronic devices, and the numerically calculated results for a practical case are provide an understanding of the transport characteristics of the piezotronic transistors. The theory presented here not only establishes the solid physical background for piezotronics, but also provides theoretical support to guide experimental design of piezotronic devices.

Acknowledgements

This research was supported by BES DOE (DE-FG02-07ER46394).

Received: March 10, 2011
Published online:

[1] Z. W. Pan, Z. R. Dai, Z. L. Wang, *Science* **2001**, *291*, 1947.
[2] W. Lu, C. M. Lieber, *J. Phys. D: Appl. Phys.* **2006**, *39*, R387.
[3] C. M. Lieber, Z. L. Wang, *MRS Bull.* **2007**, *32*, 99.
[4] Z. L. Wang, *Adv. Mater.* **2007**, *19*, 889.
[5] Z. L. Wang, *Adv. Funct. Mater.* **2008**, *18*, 3553.
[6] Z. L. Wang, *Mat. Sci. Eng. R* **2009**, *64*, 33.
[7] Z. L. Wang, *J. Phys. Chem. Lett.* **2010**, *1*, 1388.
[8] Z. L. Wang, J. H. Song, *Science* **2006**, *312*, 242.
[9] X. D. Wang, J. H. Song, J. Liu, Z. L. Wang, *Science* **2007**, *316*, 102.
[10] Y. Qin, X. D. Wang, Z. L. Wang, *Nature* **2008**, *451*, 809.
[11] X. D. Wang, J. Zhou, J. H. Song, J. Liu, N. S. Xu, Z. L. Wang, *Nano Lett.* **2006**, *6*, 2768.
[12] J. H. He, C. L. Hsin, J. Liu, L. J. Chen, Z. L. Wang, *Adv. Mater* **2007**, *19*, 781.
[13] C. S. Lao, Q. Kuang, Z. L. Wang, M. C. Park, Y. L. Deng, *Appl. Phys. Lett.* **2007**, *90*, 262107.
[14] Y. F. Hu, Y. L. Chang, P. Fei, R. L. Snyder, Z. L. Wang, *ACS Nano* **2010**, *4*, 1234.
[15] Y. F. Hu, Y. Zhang, Y. L. Chang, R. L. Snyder, Z. L. Wang, *ACS Nano* **2010**, *4*, 4220.
[16] Z. L. Wang, *Nano Today* **2010**, *5*, 540.
[17] Y. Gao, Z. L. Wang, *Nano Lett.* **2007**, *7*, 2499.
[18] Y. Gao, Z. L. Wang, *Nano Lett.* **2009**, *9*, 1103.
[19] a) S. M. Sze, *Physics of semiconductor devices*, 2nd ed., Wiley, New York **1981**; b) W. Schottky, *Naturwissenschaften* **1938**, *26*, 843; c) H. A. Bethe, *MIT Radiat. Lab. Rep.* **1942**, *43*, 12; d) C. R. Crowell, S. M. Sze, *Solid-State Electron.***1966**, *9*, 1035.
[20] T. Ikeda, *Fundamentals of Piezoelectricity*, Oxford University Press, Oxford, UK **1996**.
[21] G. A. Maugin, *Continuum Mechanics of Electromagnetic Solids*, North-Holland, Amsterdam **1988**.
[22] R. W. Soutas-Little, *Elasticity, XVI, 431*, Dover Publications, Mineola, NY **1999**.
[23] W. Wu, Y. Wei, Z. L. Wang, *Adv. Mater.* **2010**, *22*, 4711.
[24] Comsol Model Gallery (Semiconductor Diode), http://www.comsol.com/showroom/gallery/114/, accessed April 2011.
[25] S. Selberherr, *Analysis and Simulation of Semiconductor Devices*, Springer-Verlag, New York **1984**.